Journal of Molecular Structure 1149 (2017) 149–154

Contents lists available at ScienceDirect

Journal of Molecular Structure

journal homepage: http://www.elsevier.com/locate/molstruc

Synthesis, structure, and magnetic properties of a dinuclear antiferromagnetically coupled iron(II) complex

Fatima Setifi [a, *], Piotr Konieczny [b, **], Christopher Glidewell [c], Mina Arefian [d], Robert Pelka [b], Zouaoui Setifi [a, e], Masoud Mirzaei [d, ***]

[a] Laboratoire de Chimie, Ingénierie Moléculaire et Nanostructures (LCIMN), Université Ferhat Abbas Sétif 1, Sétif, 19000, Algeria
[b] The H. Niewodniczański Institute of Nuclear Physics, Polish Academy of Sciences, Radzikowskiego 152, 31-342, Kraków, Poland
[c] School of Chemistry, University of St Andrews, Fife, KY16 9ST, United Kingdom
[d] Department of Chemistry, Faculty of Science, Ferdowsi University of Mashhad, Mashhad, 91775-1436, Iran
[e] Département de Technologie, Faculté de Technologie, Université 20 Août 1955-Skikda, Skikda, 21000, Algeria

ARTICLE INFO

Article history:
Received 20 June 2017
Received in revised form
25 July 2017
Accepted 26 July 2017
Available online 27 July 2017

Keywords:
Dinuclear iron(II) complex
1,4-tpbd
Antiferromagnetism
Hydrothermal synthesis
Crystal structure

ABSTRACT

A new dinuclear Fe(II) complex with the general formula $[Fe_2(1,4\text{-tpbd})(dca)_4(H_2O)_2]$ (**1**) (in which 1,4-tpbd = *N,N,N′,N′*-tetrakis(2-pyridylmethyl)benzene-1,4-diamine; dca = dicyanamide, $[N(CN)_2]^-$), has been prepared under hydrothermal conditions and fully characterized by elemental analysis, infrared spectroscopy, X-ray diffraction, and magnetic measurements. The compound crystallizes in the triclinic system and *P*-1 space group with $Z = 1$ and the following unit cell parameters: $a = 8.165(5)$ Å, $b = 10.236(5)$ Å, $c = 13.105(5)$ Å, $\alpha = 81.421(5)^\circ$, $\beta = 78.810(5)^\circ$, $\gamma = 72.941(5)^\circ$, and $V = 1022.2(9)$ Å^3. The Fe(II) ions are six-coordinated, in distorted octahedral fashion, by three N atoms of tpbd ligand, one water oxygen atom and two N atoms of two dicyanamide anions. The intra-dinuclear Fe···Fe distance via the bridged μ_2-tpbd ligand is 8.293(8) Å. In the molecular arrangement, the combination of O–H···N and C–H···N hydrogen bonds links the title complex to form a three-dimensional supramolecular structure. Magnetic susceptibility measurements (2–300 K) show that **1** presents weak antiferromagnetic exchange between the two nearest Fe^{2+} ions with the coupling constant $J = -1.05$ cm^{-1}.

© 2017 Elsevier B.V. All rights reserved.

1. Introduction

Spin crossover (*SCO*) compounds are a widely studied family in which external stimuli like temperature, pressure or laser light irradiation (LIESST effect: Light-Induced Excited Spin-State Trapping) can induce a transition between two spin states [1–3]. In case of 3d ions the proper balance between the ligand field and the pairing energy plays a crucial role for this effect [4]. The most intensively studied *SCO* compounds are based on Fe(II) ($3d^6$), in which the magnetic properties can dramatically change from a paramagnetic high-spin state (HS, S = 2) to a diamagnetic low-spin state (LS, S = 0) [5,6].

The great interest in *SCO* complexes is associated with their potential applications as data storage media, molecular switches or guest dependent sensors [7–9]. Although much work has been published in this area there are still many problems to be solved including, for instance, those involving wide hysteresis loops at room temperature [10], multi-step hysteresis [11], multifunctional *SCO* [12] and how these properties correlate with structure [13–15].

Aiming to contribute to the *SCO* magneto-chemistry, we have focused our efforts mainly on searching for new *SCO* systems based on Fe ions. For this purpose we have synthesized a novel dinuclear Fe(II) complex with the polypyridyl 1,4-tpbd ligand. The resulting complex $[Fe_2(1,4\text{-tpbd})(dca)_4(H_2O)_2]$ (**1**) unfortunately does not show the crossover effect, however, we believe that the synthesis of this compound represents a significant step towards obtaining the desired bistable complexes.

Here we present the synthesis, structure and magnetic properties of **1**. We have also used the magnetic data to calculate the strength of exchange coupling between the Fe(II) ions.

* Corresponding author.
** Corresponding author.
*** Corresponding author.
E-mail addresses: fat_setifi@yahoo.fr (F. Setifi), piotr.konieczny@ifj.edu.pl (P. Konieczny), mirzaeesh@um.ac.ir (M. Mirzaei).

http://dx.doi.org/10.1016/j.molstruc.2017.07.085
0022-2860/© 2017 Elsevier B.V. All rights reserved.

2. Experimental

2.1. Materials and physical measurements

Chemical reagents were purchased commercially and were used as received without further purification. Elemental analyses (C, H and N) were performed using a Perkin-Elmer 2400 series II CHN analyzer. The ligand 1,4-tpbd (1,4-tpbd = *N,N,N′N′*-tetrakis(2-pyridylmethyl)benzene-1,4-diamine) was prepared according to the literature method [16]. Infrared (IR) spectrum was recorded in the range 4000–500 cm^{-1} on a FT-IR Bruker ATR Vertex 70 Spectrometer.

Magnetic susceptibility measurements of polycrystalline samples were measured over the temperature range 2–300 K with a Quantum Design MPMSXL7 SQUID magnetometer with applied magnetic field of 500 Oe. The isothermal magnetization measurements were performed at 2.0 K in a magnetic field range ±70 kOe. Data were corrected for the diamagnetic contribution calculated from Pascal's constants [17].

2.2. Synthesis and crystal growth

A mixture of $FeSO_4.7H_2O$ (0.2 mmol, 56 mg), 1,4-tpbd (0.1 mmol, 47 mg) and Nadca (0.4 mmol, 36 mg) in water–methanol (4:1 v/v, 20 mL) was heated at 453 K for 2 days in a sealed Teflon-lined stainless steel vessel under autogenous pressure and then gradually cooled to room temperature at a rate of 10 K h^{-1}. After the reaction vessels had cooled to ambient temperature, orange crystals were collected by filtration. (**1**) yield 33%. Elemental analysis data: Anal. Calc. (%) for $C_{38}H_{32}Fe_2N_{18}O_2$ (M, 884.51 g/mol): C, 51.60; H, 3.65; N, 28.50. Found: C, 51.45; H, 3.58; N, 28.87%. Main IR bands (ν/cm^{-1}): ν_s(C≡N) 2168(vs); ν_{as}(C≡N) 2232(m); ν_s(C≡N) + ν_s(C≡N) 2296 (m).

2.3. X-ray crystallographic studies

A single crystal study of **1** was performed at 296 K using a Bruker APEX-II diffractometer equipped with a CCD area detector with graphite-monochromated Mo-Kα radiation (λ = 0.71073 Å) generated from a sealed tube source. Data collection, indexing with reduction and absorption corrections were performed using APEX2, SAINT and SADABS programs, respectively [18,19]. The structure was solved by direct methods using SHELXS-97 [20] and refined by full-matrix least squares on F^2 with all data, using SHELXL-2014 [21]. The refinement was handled [21,22] as a non-merohedral twin with twin matrix (−1,0,0/0,-1,0/−0.528,-0.258,1). All H atoms were located in difference maps. The H atoms bonded to C atoms were then treated as riding atoms in geometrically idealised positions with C–H distances 0.93 Å (aromatic and pyridyl) or 0.97 Å (CH_2) and with $U_{iso}(H) = 1.2\ U_{eq}(C)$. The H atoms bonded to the O atoms were permitted to ride at the positions located in difference maps, with $U_{iso}(H) = 1.5\ U_{eq}(O)$, giving O–H distances of 0.96 Å. Both of the two independent dca ligands were disordered over two sets of atomic sites having unequal occupancies in each case. For the minor components, the bonded distances and the 1.3 non-bonded distances were restrained to have the same values as the corresponding distances in the major components, subject to S.U. values of 0.005 Å and 0.01 Å respectively. In addition, the anisotropic displacement parameters for pairs of partial occupancy atoms occupying effectively the same volume of physical space were constrained to be identical. Subject to these conditions, the occupancies for the dca components containing atoms N31 and N51 refined to 0.83(4) and 0.17(4) respectively, and those for the dca ligands containing atoms N41 and N61 refined to 0.89(3) and 0.11(3). The final refined twin fractions were 0.390(5) and 0.610(5).

The crystallographic data and experimental details for structural analyses are summarized in Table 1.

3. Result and discussion

3.1. Infrared spectroscopy

The IR spectrum of **1** shows strong to medium absorptions in the 2296–2168 cm^{-1} region corresponding to the ν(C≡N) stretching frequencies of the dca ligand [23]. The spectrum of the title compound is given as Supplementary material (Fig. S1).

3.2. Crystal structure description

The crystal structure of the compound **1** is shown in Fig. 1. Single-crystal X-ray diffraction analyses reveal that **1** crystallizes in the space group *P*-1 with half of a $[Fe_2(1,4\text{-tpbd})(dca)_4(H_2O)_2]$ dimer in the asymmetric unit. The dinuclear complex (**1**) consists of an N,N,N′,N′-tetrakis(2-pyridylmethyl)benzene-1.4diamine (1,4-tpbd) component coordinated to two $[Fe(dca)_2(OH_2)]$ units, where dca represents the dicyanamide anion $[N(CN)_2]^-$. The 1,4-tpbd unit lies across a center of inversion, chosen for the reference complex as that at (½, ½, ½), so that the two Fe(II) centers are equivalent by symmetry. The three N atoms at each end of the 1,4-tpbd adopt a facial configuration, as do the dca and the water molecule. One of two pyridyl N atoms is trans to the water ligand and the other is trans to one of the dca ligand, while the N bonded to the aryl ring is trans to the other dca ligand. The two independent dca units are both disordered over two sets of atomic sites having occupancies 0.83(4) and 0.17(4) for one, and 0.89(3) and 0.11(3) for the other.

As depicted in Fig. 2, complex **1** possesses distorted octahedral coordination geometry. Each Fe(II) ion is thus coordinated by three N atoms from the 1,4-tpbd ligand, one N atom from each of the dca ligands and one H_2O molecule with bond distances ranging from 2.094(8) Å to 2.359(7) Å, which are in good agreement with previous reported values for Fe–N and Fe–O bond lengths [24,25]. The bond distances to the Fe(II) center in **1** are almost all greater than 2.1 Å, and all are similar to the corresponding distances in the high

Table 1
Crystallographic data and refinement parameters for complex **1**.

1	
Empirical formula	$C_{38}H_{32}Fe_2N_{18}O_2$
Formula weigh	884.52
Temperature/K	296(2)
Crystal system	triclinic
Space group	*P*-1
a/Å	8.165 (5)
b/Å	10.236 (5)
c/Å	13.105 (5)
α/°	81.421 (5)
β/°	78.810 (5)
γ/°	72.941 (5)
V/Å^3	1022.2 (9)
Z	1
D_{calcd}/g cm^{-3}	1.437
Radiation type	Mo-*Kα*
μ/mm^{-1}	0.768
F(000)	454
$2\theta_{max}$ /°	25.5
Ref. coll., ind., $I > 2\sigma(I)$	15771, 3755, 3093
R_{int}	0.109
No. of parameters	298
GOOF	1.092
R_1, wR_2 [$I > 2\sigma(I)$]	0.086, 0.259
$\Delta\rho_{max}$/e Å	1.30
$\Delta\rho_{min}$/e Å	−1.14

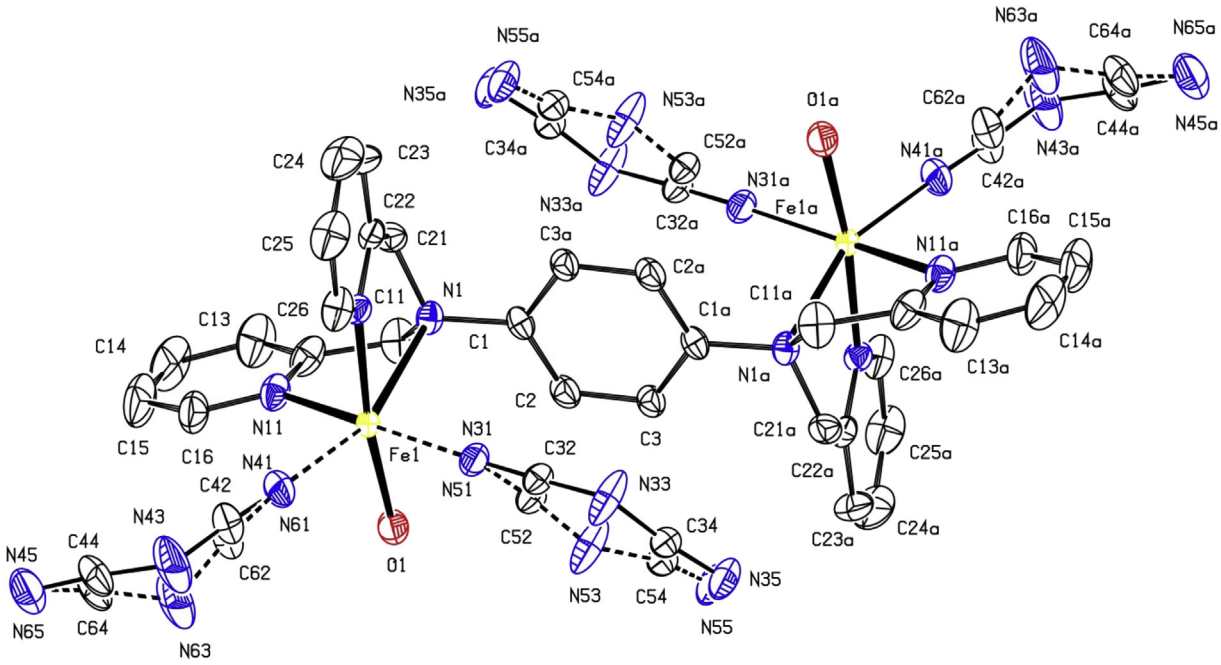

Fig. 1. The molecular structure of the title complex with the atom numbering scheme. Displacement ellipsoids are drawn at the 30% probability level, and the atoms marked 'a' are at the symmetry position (1−x, 1−y, 1−z). For the sake of clarity, the H atoms have been omitted.

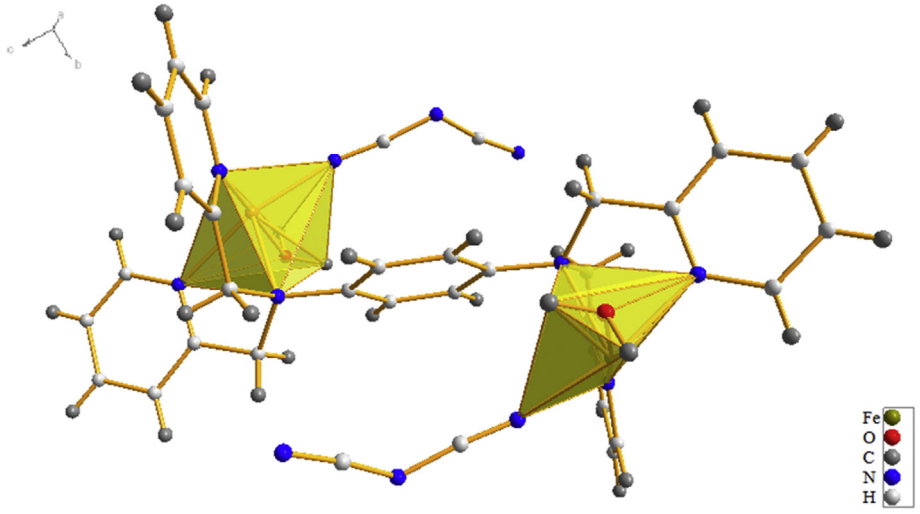

Fig. 2. Polyhedral presentation of distorted coordination sphere around Fe(II) centers.

spin complexes [26]. On the other hand the distances to the pyridyl N atoms in **1** are ca. 0.2 Å longer than those corresponding Fe–N distances in the low-spin Fe(II) complexes [27] which are closely clustered around 1.97 Å. On this basis, we deduce from the structural metrics that at ambient temperature complex **1** adopts a high-spin configuration, corresponding in approximate octahedral microsymmetry to a $^5T_{2g}$ state. The Fe···Fe distance within the

Table 2
Selected bond lengths (Å) and bond angles (°) for compound **1.**

bond lengths (Å)		bond angles (°)			
Fe1–N31	2.104(8)	O1–Fe1–N1	96.3(3)	N11–Fe1–N31	167.1(3)
Fe1–O1	2.135(9)	O1–Fe1–N11	81.2(3)	N21–Fe1–N31	90.1(3)
Fe1–N1	2.359(7)	O1–Fe1–N21	171.0(3)	N41–Fe–O1	95.1(3)
Fe1–N11	2.214(8)	O1–Fe1–N31	89.3(3)	N41–Fe1–N21	93.9(3)
Fe1–N21	2.143(7)	N1–Fe1–N11	72.9(3)	N41–Fe1–N1	193.7(3)
Fe1–N41	2.094(8)	N1–Fe1–N21	74.9(2)	N41–Fe1–N31	95.9(3)
		N1–Fe1–N31	99.7(3)	N41–Fe1–N1	160.8(3).
		N11–Fe1–N21	97.8(3)		

Table 3
Hydrogen bond lengths (Å) and angles (°) of **1.**

D-H···A	D-H	H···A	D···A	D-H···A
O1–H1A···N45^{i}	0.96	2.18	2.738(18)	116
O1–H1A···N65^{i}	0.96	1.96	2.64(12)	127
O1–H1B···N35^{ii}	0.96	1.98	2.774(19)	139
O1–H1B···N55^{ii}	0.96	1.85	2.73(10)	150
C13–H13···N45^{iii}	0.93	2.62	3.52(2)	163

Symmetry codes: (i) −x, 2−y, −z; (ii) −x, 1−y, 1−z; (iii) 1 + x, −1 + y, z.

centrosymmetric complex is 8.293(8) Å. The strain caused by 1,4-tpbd chelating ligand results in a distortion of the coordination geometry from the octahedral ideal with observed angles between mutually cis coordination sites ranging from 72.9(3)° to 99.7(3)° (Table 2).

Molecules of the dinuclear complex (**1**) are linked by O–H···N hydrogen bonds (Table 3) to form sheets lying parallel to (011) containing centrosymmetric rings of $R^2_2(16)$ and $R^4_4(42)$ types (Fig. 3), and these sheets are further linked by a C–H···N hydrogen bond to form a continuous three-dimensional framework structure.

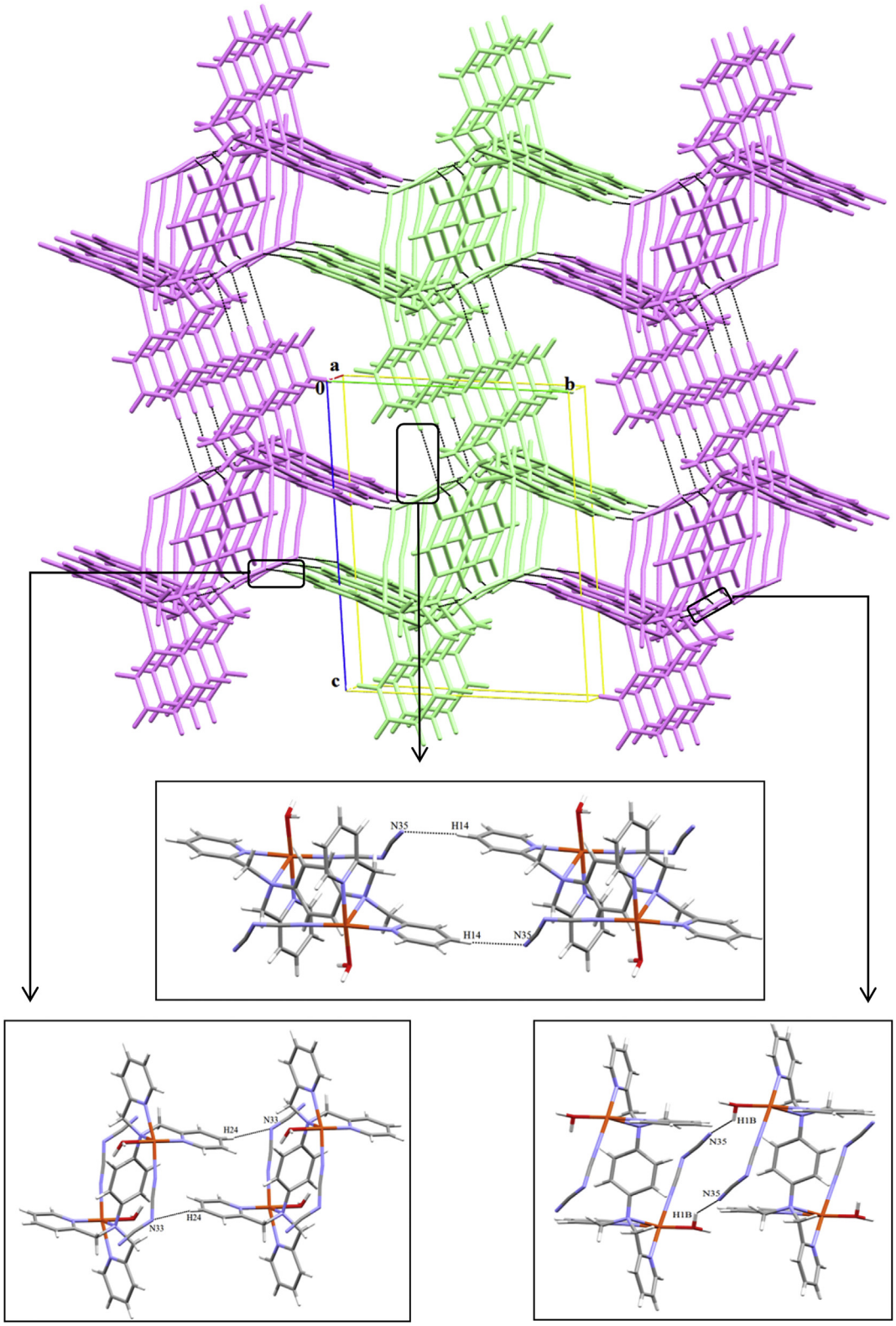

Fig. 3. Packing diagram of complex **1**, and specific hydrogen bond interactions separately in detail.

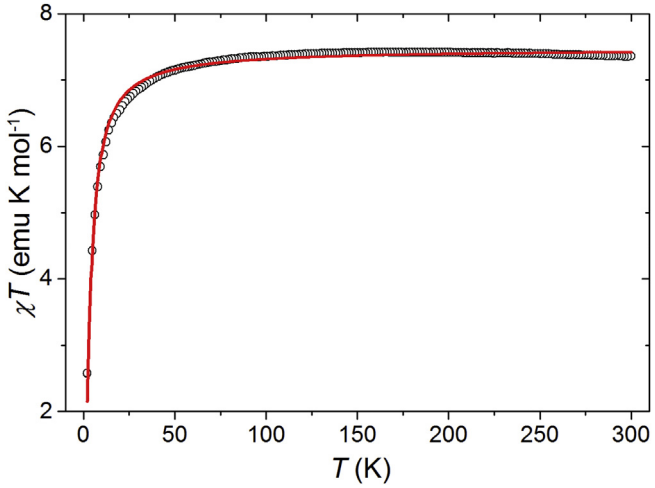

Fig. 4. The χT vs. T plot of **1** at $H = 500$ Oe. The black empty circles are the measured data points. The red solid line stands for the best fit of χT data according to the HDVV Hamiltonian for dinuclear compounds. (For interpretation of the references to colour in this figure legend, the reader is referred to the web version of this article.)

3.3. Magnetic properties

Fig. 4 shows the χT versus temperature plot, where the value of χT is almost constant from room temperature down to 100 K. On cooling further, the χT product decreases to 2.58 emu K mol^{-1} at 2.0 K. To estimate the magnetic coupling between iron ions inside the dimer, the experimental data were fitted using the Heisenberg-Dirac-Van Vleck Hamiltonian:

$$\widehat{H} = -J\widehat{S}_{Fe1}\widehat{S}_{Fe2} + \mu_B g\left(\widehat{S}_{Fe1} + \widehat{S}_{Fe2}\right)H$$

where the first term describes the exchange coupling between iron ions and the second term represents the Zeeman splitting effect. The best fit is shown in Fig. 4 as solid line and the derived parameters are $J = -1.05$ cm^{-1} and $g = 2.23$, assuming that the Fe(II) ions are in the high spin state at room temperature with $S_{Fe} = 2.0$ (see Fig. 5).

The negative value of J indicates a weak antiferromagnetic coupling, and the value of g was used to calculate free-ion contribution from two HS Fe(II) ions which amounted to 7.46 emu K mol^{-1}. This is slightly higher than the value of χT at room temperature for compound **1** which was determined as 7.36 emu K mol^{-1}. The Curie-Weiss fit of inverse susceptibility as a function of temperature yields Curie constant 7.44 emu K mol^{-1}, close to the measured room temperature value of χT and the calculated free-ion contribution. The negative Weiss constant $\theta = -1.06$ K confirms the antiferromagnetic character of magnetic interactions. The isothermal magnetization data at 2.0 K are shown in Fig. 6. In a field of 70 kOe, the magnetization reaches the value of 6.05 μ_B and does not reveal saturation.

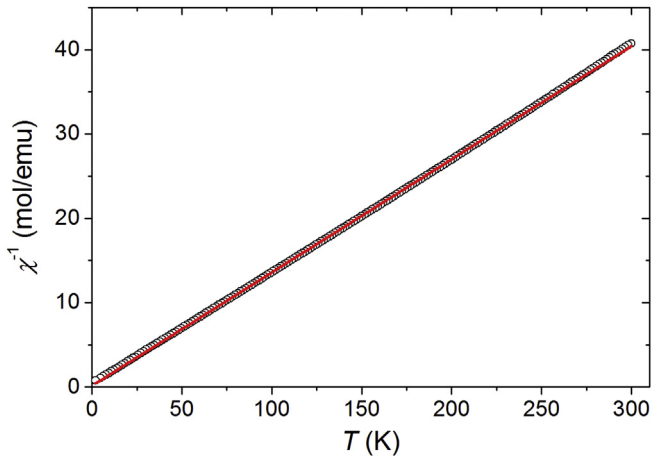

Fig. 5. Thermal variation of the inverse magnetic susceptibility χ^{-1} (black empty circles) with the Curie-Weiss fit (red solid line). (For interpretation of the references to colour in this figure legend, the reader is referred to the web version of this article.)

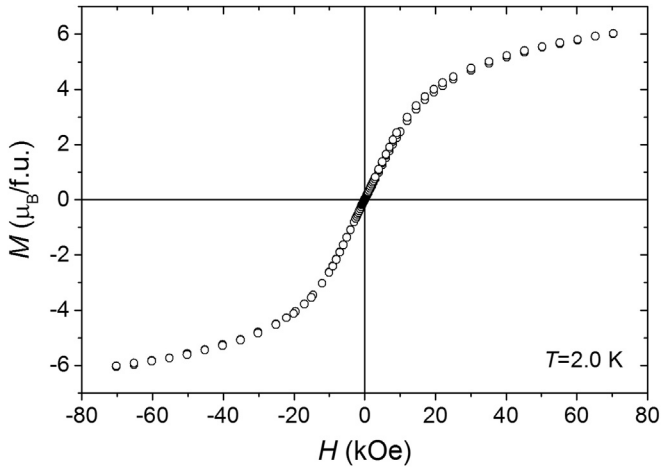

Fig. 6. Field dependence of isothermal magnetization at $T = 2.0$ K.

4. Conclusions

In summary, the centrosymmetric dinuclear compound formulated as $[Fe_2(1,4\text{-tpbd})(dca)_4(H_2O)_2]$ is reported. Synthesis, characterization, magnetic properties and its supramolecular 3D structure are also presented in detail. The dinuclear tpbd bridged Fe(II) compound displays a weak antiferromagnetic interaction between the two HS (high spin) Fe centers with a coupling constant J of -1.05 cm^{-1}.

Acknowledgements

The authors are indebted to the Algerian DGRSDT (Direction Générale de la Recherche Scientifique et du Développement Technologique) and Université Ferhat Abbas Sétif 1 for financial support.

Appendix A. Supplementary data

Supplementary data related to this article can be found at http://dx.doi.org/10.1016/j.molstruc.2017.07.085.

References

[1] P. Gutlich, H.A. Goodwin, Spin crossover-an overall perspective, in: Spin Crossover Transit. Met. Compd. I, Springer, Berlin, Heidelberg, 2004, pp. 1–47, http://dx.doi.org/10.1007/b13527.
[2] J.-F. Létard, L. Capes, G. Chastanet, N. Moliner, S. Létard, J.-A. Real, O. Kahn, Critical temperature of the LIESST effect in iron(II) spin crossover compounds, Chem. Phys. Lett. 313 (1999) 115–120, http://dx.doi.org/10.1016/S0009-2614(99)01036-2.
[3] J.A. Real, A.B. Gaspar, M.C. Muñoz, Thermal, pressure and light switchable spin-crossover materials, Dalton Trans. (2005) 2062–2079, http://dx.doi.org/10.1039/b501491c.

[4] S. Brooker, Spin crossover with thermal hysteresis: practicalities and lessons learnt, Chem. Soc. Rev. 44 (2015) 2880–2892, http://dx.doi.org/10.1039/c4cS00376d.
[5] J.A. Real, A.B. Gaspar, V. Niel, M.C. Muñoz, Communication between iron(II) building blocks in cooperative spin transition phenomena, Coord. Chem. Rev. 236 (2003) 121–141, http://dx.doi.org/10.1016/S0010-8545(02)00220-5.
[6] R. Adam, R. Ballesteros-Garrido, S. Ferrer, B. Abarca, R. Ballesteros, J.A. Real, M.C. Muñoz, From six-coordinate to eight-coordinate iron (II) complexes with pyridyltriazolo-pyridine frameworks, CrystEngComm 18 (2016) 7950–7954, http://dx.doi.org/10.1039/C6CE01540A.
[7] O. Kahn, Spin-transition polymers: from molecular materials toward memory devices, Science 279 (1998) 44–48, http://dx.doi.org/10.1126/science.279.5347.44.
[8] J.-F. Létard, P. Guionneau, L. Goux-Capes, Towards Spin Crossover Applications, in: Spin Crossover Transit. Met. Compd. III, Springer-Verlag, Berlin/Heidelberg, n.d.: pp. 221–249. http://dx.doi.org/10.1007/b95429.
[9] A. Bousseksou, G. Molnár, P. Demont, J. Menegotto, Observation of a thermal hysteresis loop in the dielectric constant of spin crossover complexes: towards molecular memory devices, J. Mater. Chem. 13 (2003) 2069–2071, http://dx.doi.org/10.1039/B306638J.
[10] G. Gallé, D. Deldicque, J. Degert, Th Forestier, J.-F. Létard, E. Freysz, Room temperature study of the optical switching of a spin crossover compound inside its thermal hysteresis loop, Appl. Phys. Lett. 96 (2010) 041907, http://dx.doi.org/10.1063/1.3294312.
[11] J. Olguín, S. Brooker, Spin-crossover in discrete polynuclear complexes, in: Spin- Crossover Materials: Properties and Applications, John Wiley & Sons Ltd, Oxford, UK, 2013, pp. 77–120, http://dx.doi.org/10.1002/9781118519301.ch3.
[12] F.J. Valverde-Muñoz, M. Seredyuk, M.C. Muñoz, K. Znovjyak, I.O. Fritsky, J.A. Real, Strong cooperative spin crossover in 2D and 3D Fe II –M I,II Hofmann-like coordination polymers based on 2-Fluoropyrazine, Inorg. Chem. 55 (2016) 10654–10665, http://dx.doi.org/10.1021/acs.inorgchem.6b01901.
[13] M.A. Halcrow, Structure:function relationships in molecular spin-crossover complexes, Chem. Soc. Rev. 40 (2011) 4119–4142, http://dx.doi.org/10.1039/C1CS15046D.
[14] A. Bousseksou, G. Molnár, J.A. Real, K. Tanaka, Spin crossover and photomagnetism in dinuclear iron(II) compounds, Coord. Chem. Rev. 251 (2007) 1822–1833, http://dx.doi.org/10.1016/j.ccr.2007.02.023.
[15] A. Bousseksou, G. Molnar, J.A. Real, K. Tanaka, Spin crossover and photomagnetism in dinuclear iron(II) compounds, Coord. Chem. Rev. 251 (2007) 1822–1833, http://dx.doi.org/10.1016/j.ccr.2007.02.023.
[16] T. Buchen, A. Hazell, L. Jessen, C.J. McKenzie, L.P. Nielsen, J.Z. Pedersen, D. Schollmeyer, Copper complexes of a p-phenylenediamine-based bis(-tridentate) ligand, J. Chem. Soc. Dalt. Trans. (1997) 2697–2704, http://dx.doi.org/10.1039/a701588g.
[17] G.A. Bain, J.F. Berry, Diamagnetic corrections and Pascal's constants, J. Chem. Educ. 85 (2008) 532–536, http://dx.doi.org/10.1021/ed085p532.
[18] U.G.M. Sheldrick, SADABS, Bruker (Version 2.10; 2003), Bruker AXS Inc., Madison, Wisconsin, 2003. No Title.
[19] U. Bruker, APEX2 and SAINT, Bruker, Bruker AXS Inc., Madison, Wisconsin, 2009. No Titl.
[20] G.M. Sheldrick, A short history of SHELX, Acta Crystallogr. Sect. A Found. Crystallogr. 64 (2008) 112–122, http://dx.doi.org/10.1107/S0108767307043930.
[21] G. M. Sheldrick, Crystal structure refinement with SHELXL, Acta Crystallogr. Sect. C Struct. Chem. 71 (2polyhe015) 3–8. http://dx.doi.org/10.1107/S2053229614024218.
[22] A.L. Spek, Structure validation in chemical crystallography, Acta Crystallogr. Sect. D. Biol. Crystallogr. 65 (2009) 148–155, http://dx.doi.org/10.1107/S090744490804362X.
[23] G.A. van Albada, S. Tanase, A. Mohamadou, I. Mutikainen, U. Turpeinen, J. Reedijk, Synthesis, structure and magnetism of two new polymeric double dicyanamido-bridged Mn(II) compounds, Polyhedron 25 (2006) 2236–2240, http://dx.doi.org/10.1016/j.poly.2006.01.022.
[24] F. Reuter, E. Rentschler, Structural, magnetic and electronic characterization of an isostructural series of dinuclear complexes of 3d metal ions bridged by tpbd, Polyhedron 52 (2013) 788–796, http://dx.doi.org/10.1016/j.poly.2012.07.050.
[25] K. Deniel, K. Nebbali, N. Cosquer, F. Conan, C.J. Gómez-García, S. Yefsah, S. Triki, Polypyridyl-based Cu(II) coordination polymers: synthesis, structural and magnetic characterizations, Polyhedron 97 (2015) 253–259, http://dx.doi.org/10.1016/j.poly.2015.05.032.
[26] Z. Setifi, F. Setifi, H. Boughzala, A. Beghidja, C. Glidewell, Tris(2,2'-bipyridine) iron(II) bis(1,1,3,3-tetracyano-2-ethoxypropenide) dihydrate, Chiral hydrogen-bonded frameworks interpenetrate in three dimensions, Acta Crystallogr. Sect. C Struct. Chem. 70 (2014) 465–469, http://dx.doi.org/10.1107/S2053229614008092.
[27] Z. Setifi, F. Setifi, S.W. Ng, A. Oudahmane, M. El-Ghozzi, D. Avignant, Tris(1,10-phenanthroline-κ^2N,N')iron(II) bis(1,1,3,3-tetracyano-2-ethoxypropenide) hemihydrate, Acta Crystallogr. Sect. E Struct. Rep. Online 69 (2013) m12–m13, http://dx.doi.org/10.1107/S1600536812048611.